*Section A-Research paper*
*ISSN 2063-5346*

# Guanidinium Carbonate Single Crystal Structural, Spectral, Optical, Mechanical, Thermal, and Antibacterial Studies with Cyanoacetic Acid as Solvent

**R.Subash Chandra Bose[1], K.Balasubramanian[2], R.Subramaniyan@Raja[3]**
1 Research Scholar (Reg.No.17211072131024)
1, 2 PG & Research Department of Physics, The M.D.T. Hindu College, Tirunelveli 627010, Tamilnadu, India
(Affiliated to Manonmaniam Sundaranar University, Abishekapatti, Tirunelveli 627012, Tamilnadu, India)
3 Department of Physics, KPR Institute of Engineering and Technology, Coimbatore-641407, Tamilnadu, India.
Corresponding Author Email id: subashchandrabose@mdthinducollege.org

Keywords:Organic material, slow evaporation, optical studies, mechanical studies, Laser Damage Threshold, NLO

## ABSTRACT

Slow evaporation procedures were used to create high-quality organic crystals of guanidinium carbonate (GC). The crystal crystallises into a Tetragonal system with space group $P4_12_12$. according to X-ray diffraction. The Fourier Transform Infrared Analysis verified the functional group present in the produced crystal. According to the optical analysis, the UV cutoff wavelength is around 239 nm. The developed crystal's optical band gap was discovered to be 5.34ev. The title compound's mechanical behaviour was examined using the Vicker microhardness tester. Nd:YAG laser measurements were made to determine the generated crystals' surface laser damage threshold. TGA/DTA analysis have been used to study thermal behaviour. By using the agar diffusion method, the antifungal activity was also targeted for examination against two well-known fungi, such as E. coli and Staphylococcus aureus.

Keywords: Slow Evaporation Method, Single Crystal x- ray diffraction, UV – Vis- Studies, TGA/DTA analysis

## 1. Introduction

Due to its application in optical devices such optical switches, optical modulators, optical bistable devices, electro-optical devices, etc., nonlinear optical (NLO) materials are receiving a lot of fascination. [1]. Material selection is required to produce beneficial NLO material for optical device applications. Better NLO materials may be designed, device performance could be enhanced, and new materials could be created with the aid of such knowledge. However, due to the complexity and wide range of compounds, including organic and inorganic ones, as well as - interactions, hydrogen bonds, charge transfer, and electron

transfer that characterise their solid structure, this work is particularly difficult [2]. Due to their specifically designed flexibility, wide band gap, high nonlinear coefficients, and appreciable laser damage threshold, organic NLO crystals have more advantages than inorganic material.. [3, 4]. An important aspects of organic materials is that, increasing the nonlinear polarization of this molecule requires introducing an electron donor or electron acceptor group into the organic molecules. Among the various organic compounds, Guanidinium ion can form a wide family of hydrogen-bonded crystals and this cation is relatively simple [5]. Guanidinium is a strong base material, easily reacts with most of the organic acids and gives the good crystalline product because of their six potential donor sites for hydrogen bonding interaction [6, 7].

In this article, we provide studies on the single crystal of guanidinium carbonate in the presence of cyanoacetic acid that looked at its structural, spectral, optical, mechanical, thermal, and antibacterial properties.

## 2. Experimental Procedure

### 2.1. Crystal Growth

The commercially available Guanidinium Carbonate salt (AR Grade) and Cyanoacetic acid were taken in the equimolar ratio. The calculated amount of salts was dissolved in double distilled water at room temperature. The solution stirred well for 6 h using temperature controlled magnetic stirrer to obtain saturated solution. Then the saturated solution was filtered using Whatman filter paper and allowed to evaporate at room temperature, yielded transparent crystalline salt of GC crystal. The synthesized salts were purified by repeated recrystallization and at last good transparent colorless single crystals were harvested after 45 days and shown in the fig(1)

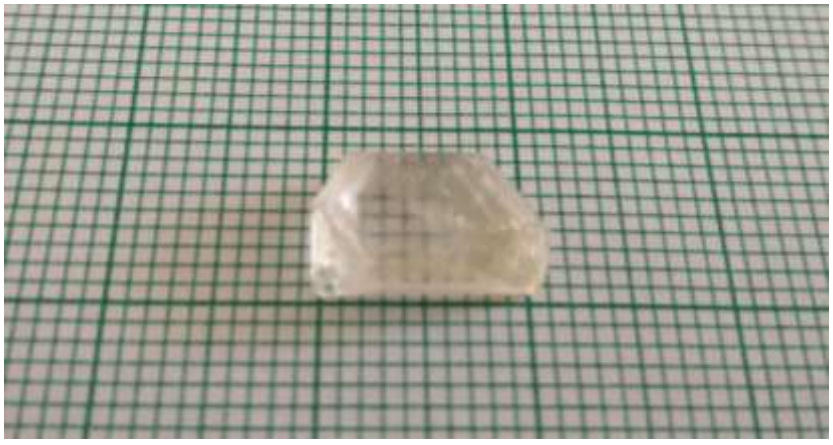

**Figure 1. As grown Guanidinium Carbonate Single Crystal**

## 3. Characterization

## 3. Results and Discussion

From the Single Crystal XRD analysis, it is confirmed that GC Crystal belongs to Tetragonal system and their space group is $P4_12_12$. The Unit cell parameters are a=6.98 Å, b=6.94 Å, c=19.65 Å and V=957 (Å) $^3$ with $\alpha=\beta=\gamma=90^0$.

### 3.1. PXRD Analysis

The well-ground powder of the generated crystal samples was analysed using powder X-ray diffraction. The data were gathered at room temperature with a source wavelength of 1.54 Å between 10°and 80° diffraction angles. The scan step time was fixed at 80 seconds and the step size of 2θ was fixed at 0.0200. The XRD pattern shows the strong diffraction peaks, confirming the good crystalline quality of the generated samples. [8]. Using the 2 values, the d-spacing of the diffraction peaks was computed. The grown crystal's indexed powder X-ray diffraction pattern is depicted in fig. (2).

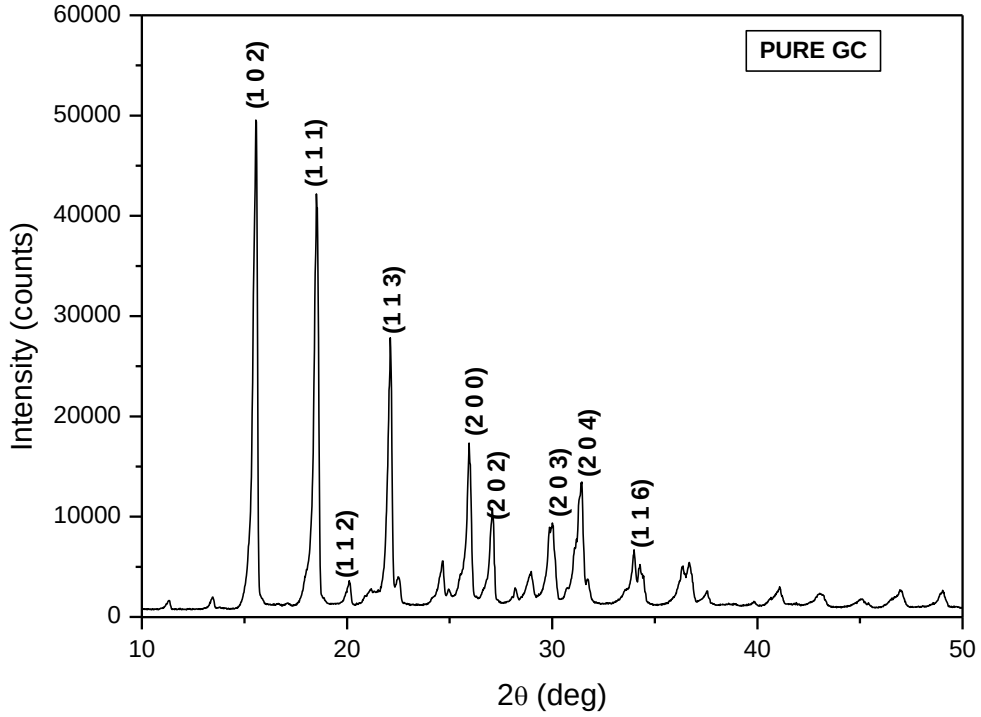


**Figure 2. PXRD Graph of Guanidinium Carbonate Single Crystal**

### 3.2. Fourier Transform Infrared Analysis

The FTIR spectrum was recorded using a Perkin Elmer FTIR Spectrum RXI Spectrometer by KBr pellet technique. Figure.3. shows the FTIR spectrum recorded in the range 400-4000 $cm^{-1}$ at room temperature. In the spectrum, the broad band centered around 3300 $cm^{-1}$ is due to C-H stretching. It overlaps with the characteristic broadband due to N-H asymmetrical absorbed at 3339 $cm^{-1}$ and 2829 $cm^{-1}$. The attributed peaks at 3268 and 3197 $cm^{-1}$ are due to stretching of O-H. [9] The presence of all functional groups of GC crystal is shown in the

table1.

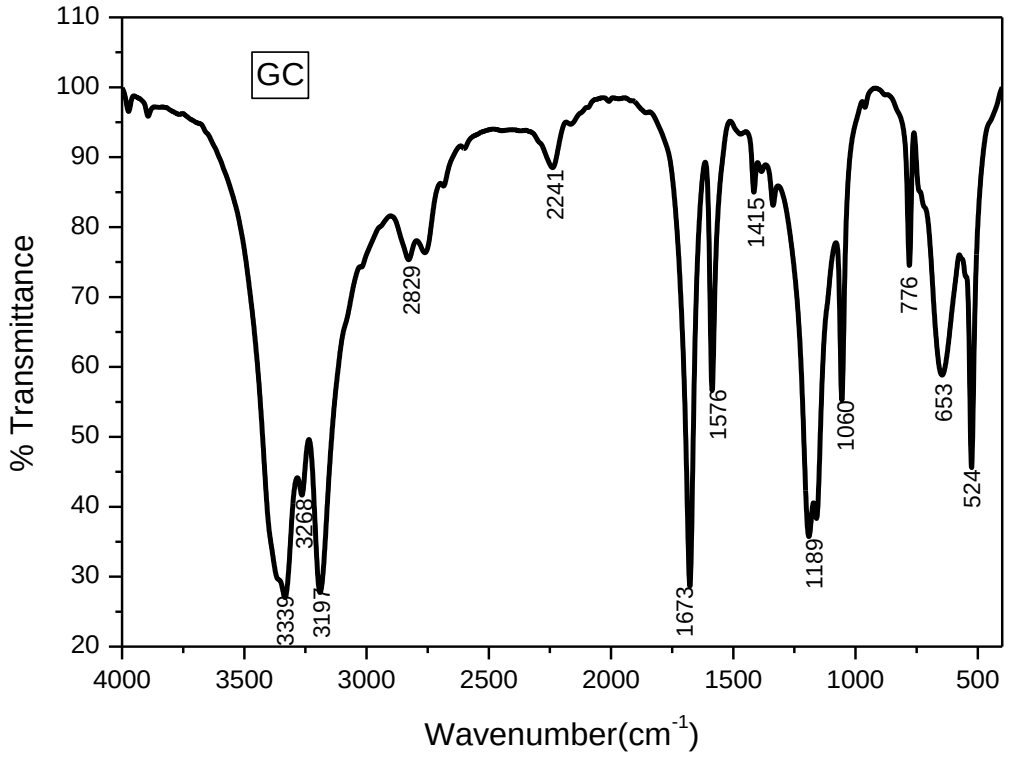


**Fig.3. FTIR Spectrum of GC**

**Table 1 Functional group assignments**

| **Wavenumber ($cm^{-1}$)** | **Assignments** | **Wavenumber ($cm^{-1}$)** | **Assignments** |
|---|---|---|---|
| 3339 | N - H Stretching | 1415 | O – H Bending (carboxylic Acid) |
| 3268 | O - H Stretching (Strong) | 1189 | C – O Stretching |
| 3197 | O - H Stretching (Weak) | 1060 | S = O Stretching |
| 2829 | N - H Stretching | 776 | C – H Bending |
| 2241 | C ≡ N Stretching | 653 | C = C Bending |
| 1673 | C = N Stretching | 524 | C – Br Stretching |
| 1576 | C = C Stretching | | |

### 3.3. Optical Characterization

#### 3.3.1. Optical absorption studies

The GC crystal's optical characteristic reveals its suitability and accountability for various device applications. Figure 4 depicts the GC crystal's UV-visible absorption spectra. Here, it is evidently not an electronic transition-related absorption. The formed crystal's lower cutoff wavelength is discovered to be 239.46 nm, and it exhibits high transparency in the visible area, indicating that it serves a

purpose in nonlinear optical applications.[10]

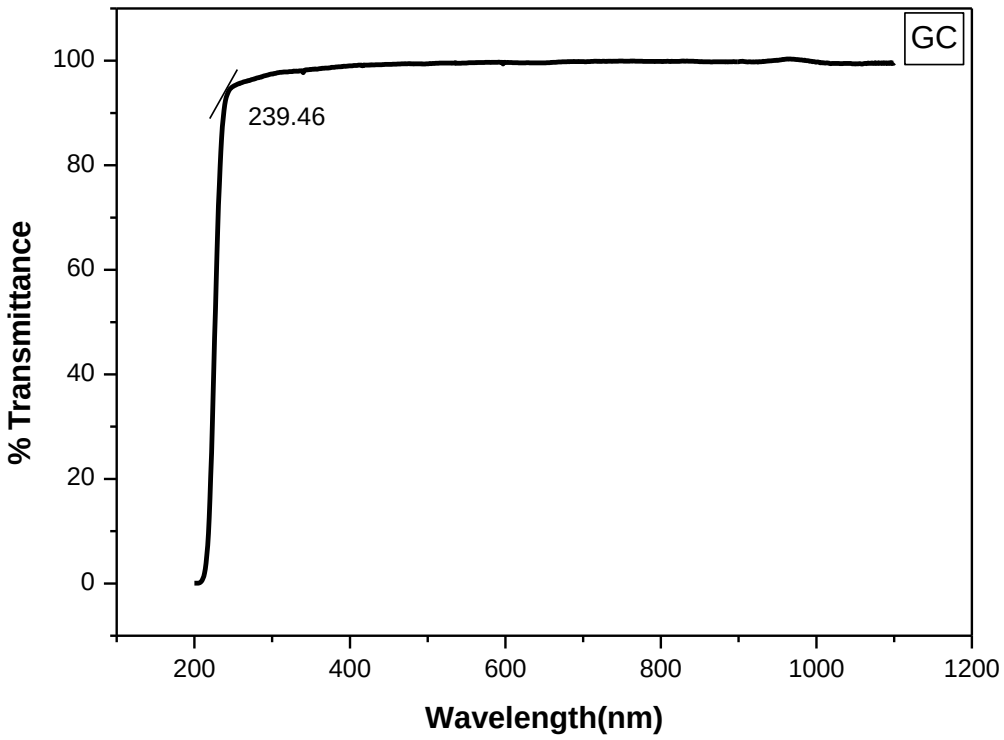


**Fig.4. Transmittance Spectrum of Grown GC Crystal**

**3.3.2. Determination of Optical Band gap**

To study the band structure and the electrons transitions of the material GC crystal has been taken for determination of optical absorption co-efficient (α) with the photon energy (E).

$$\alpha = [2.303 \log ((1/T)] / t]$$

where T is the Transmittance of the crystal, t is the thickness of the crystal.

By plotting $(\alpha h\upsilon)^2$ as a function of (hυ) as shown in the figure 5 and extrapolating the linear regions of this curve. We obtained the optical band gap of the grown crystal is 5.34 eV. This larger band gap energy of grown GC crystal proves that the crystal is insulator and have wide transmission in the visible region. This property of the grown GC crystal is used in the fabrication of many optical devices like optical switching and electro optic modulation. [11]

The absorption coefficient related to photon energy is

$$\alpha h\upsilon = \beta (h\upsilon - E_g)^n$$

Where $E_g$ is an optical energy gap and n is a number which characterizes the optical absorption process and also n has different values for different kinds of transition. There are n=1/2: direct allowed transition, n=1: non-metallic materials, n=3/2: direct forbidden transition, n=2: indirect transition, n=3: indirect forbidden transition. [12] In the present work the value of n is 1/2which exhibits that the optical transition is direct allowed transition. [13].

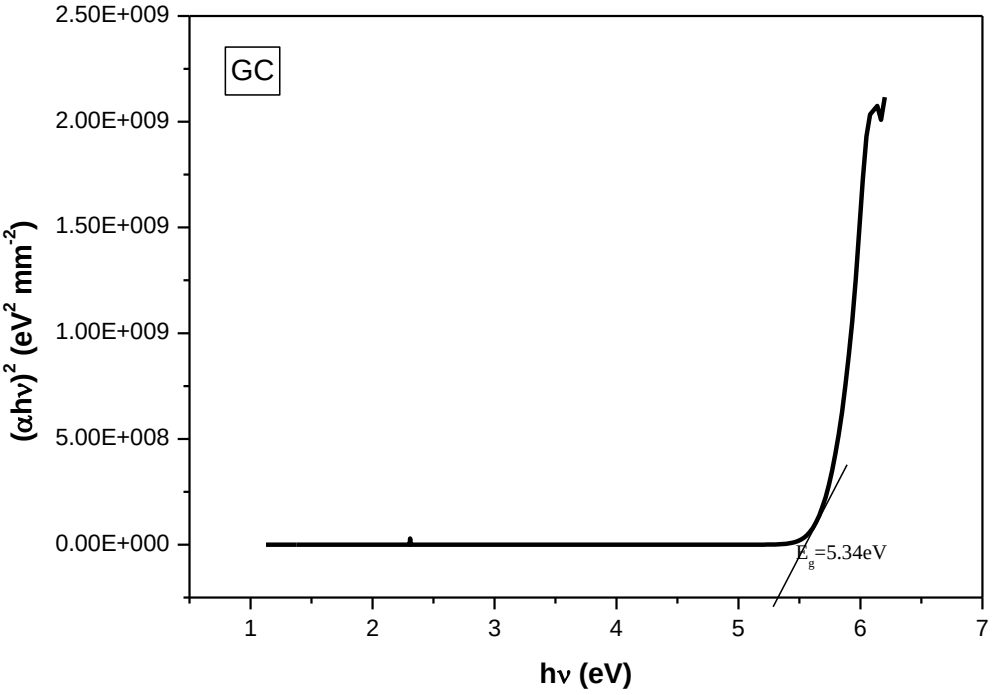


**Fig.5. Tauc Plot graph of GC Crystal**

### 3.4. Microhardness Studies

The polished Guanidinium Carbonate Single Crystal has been chosen for Vickers micro hardness. For the static indentation test, loads varying from 10 to 100 g were applied on the grown crystal using Vickers diamond pyramid indenter connected to an incident ray microscope. For each load P, an average of two impressions were recorded and the average of diagonal lengths(d) of the indentation mark after unloading was measured using a calibrated micrometer attached to the eyepiece of the microscope.

The Vickers micro hardness was calculated using the general formula,

$$H_v = 1.8544\ P / d^2\ (kg/mm^2)$$

Where P –applied load in Kg, d- diagonal length of the indentation in mm. The estimation of error in hardness value $H_v$ can be calculated using figure 6. Shows the graph of Load vs $H_v$. The hardness test could not be carried out above 100 g because crack initiation and materials chipping become significant beyond this load. The hardness of the material is found to be increases with increase in the applied indentation load. The grown crystal obeys reverse indentation size effect [14]

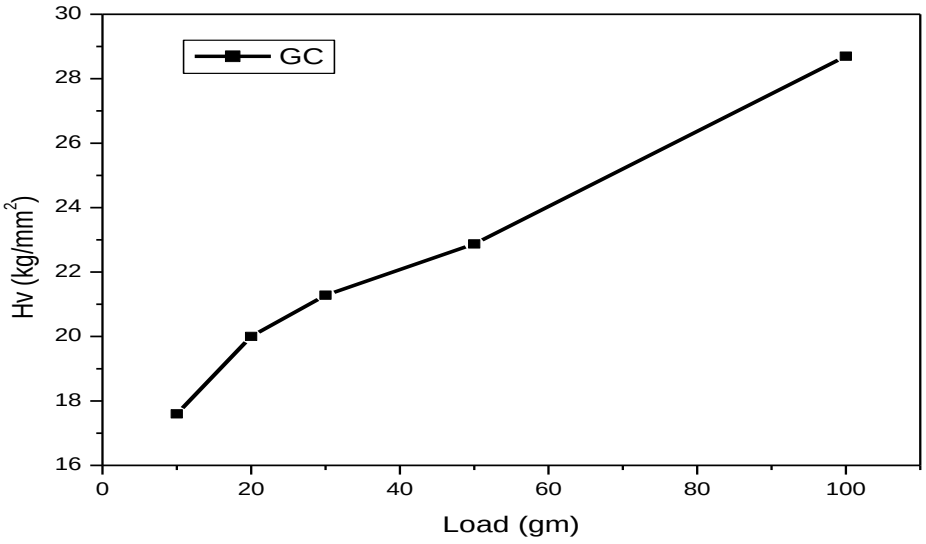


**Fig. 6. Load versus Hardness Number of GC Crystal**

The Size of indentation and the load were related using Meyer's law is given by

$$P=kd^n$$

The Slope of log (P) against log (d) plot is shown in figure 7. Which clearly agrees with the Meyer's law. The value of n (Meyer's index number) was found to be 2.50from the slope. According to Ointsch, the range $1 \leq n \leq 1.6$ for hard material, if $n \geq 1.6$ for soft material. Hence it is concluded that the GC crystal belongs to soft material. [15]

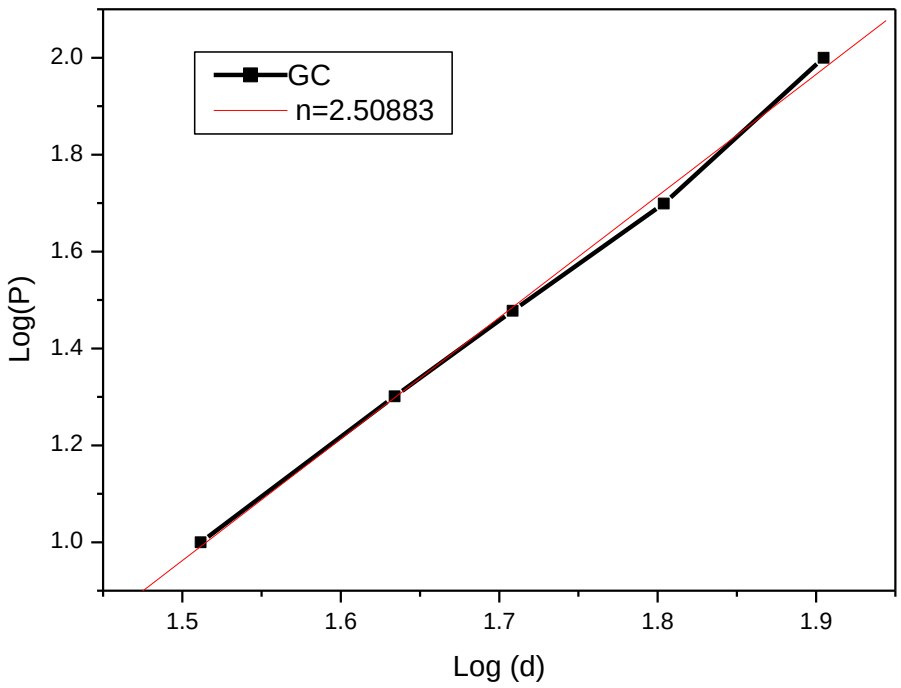


**Fig.7. Log d versus Log P graph of GC Crystal**

### 3.5. Thermal Analysis

The thermal houses of the GC crystals have been studied by the use of TG/DTA studies. This research was done for the samples to discover the weight change (TG), Energy alternate (DTA) and numerous endothermic and exothermic transitions inside the samples with the trade of temperature. The grown crystals have been placed in a closed chamber with controlled nitrogen waft environment at heating range of 5$^{o}$C/min. TG/DTA curves for GC crystals are shown in Figure 8. The TG curve provides with a quantitative measurement of mass alternate related to the transition. It shows that on melting the fabric decomposes and loses mass. From the TG diagram, GC crystal confirmed two ranges of weight loss. Thus the curve shows a gradual mass loss. From this graph, the weight reduction begins at round 139.3$^{o}$C and steps at 276.4$^{o}$C. The decomposition is likewise accompanied by using the melting of the sample at 218.4$^{o}$C as shown with the aid of DTA. The second degree of decompositions is from 276.4$^{o}$C to 409.08$^{o}$C. The residue at the stop is at 648.8$^{o}$C. From the TG study well-known shows that the sample absolutely decomposes within the first stage, the risky gases consisting of carbon, nitrogen and oxygen would have decomposed leaving in the back of a small residue [16]. Further, the crystals are observed to decompose without melting or section transformation. The TG/DTA result indicates the enough thermal balance required for a NLO crystal.

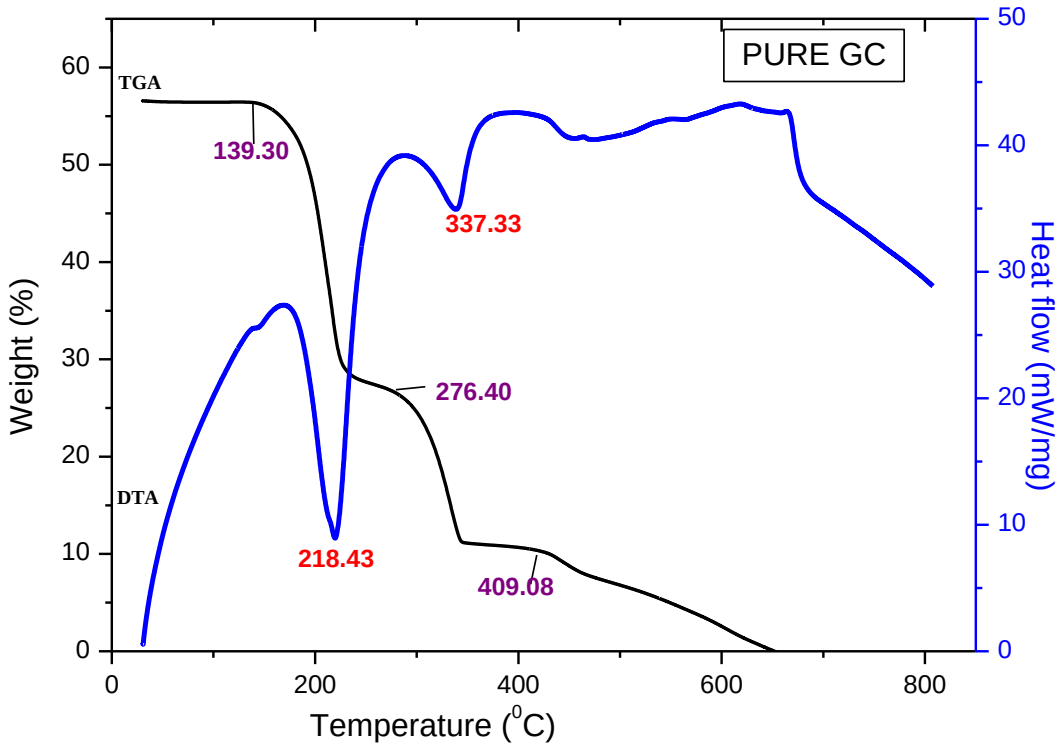


**Fig. 8. TG/DTA Curve**

### 3.6. Laser Damage threshold measurements

GC crystals were made into a rectangular slab of thickness 3mm and then the LDT was measured. A Q-switched Nd:YAG laser operating at 1064 nm radiation was

used for measurements. For this measurement 45μm diameter of the beam was focused on the crystal with 10cm focal length. At constant pulse rate of 6 ns, different magnitude of intensity was passed on the surface of GC crystal [17]. When the intensity (in mJ) of the laser beam increases, initially a dot occurs on the surface of the LA crystal. This is followed with the crack and heavy damage occurs on GC single crystal. The damage was observed at 90mJ.

### 3.7. NLO Studies

Optical damage in NLO materials may severely affect the performance of high power laser systems such as the efficiency of the optical device based on the nonlinear processes [18]. Hence high damage threshold is a significant parameter for NLO crystal. The Laser damage threshold of the Crystals was calculated using the expression

$$\textbf{Power Density (Pd)} = \frac{E}{\tau \pi r^2}$$

Where E is the energy (mJ), τ is the pulse width (ns) and r is the radius of the spot (mm). The Laser damage threshold is determined to be 9.5GW/cm$^2$ and comparisons of damage threshold for different NLO crystals are presented in Table 2. The Kurtz-Perry powder technique remains a valuable tool for initial screening of materials for second harmonic generation. KDP sample has been used as the reference material and output power intensity of GC crystal has been found to be 1.5 times higher than that of KDP crystal.

Table 1

**Comparisons of Laser damage threshold with different NLO crystals**

| Compound | SHG Efficiency | Laser Damage Threshold (GW/cm$^2$) |
|---|---|---|
| Potassium dihydrogen phosphate (KDP) | 1 | 0.2 |
| Guanidinium Carbonate** | 1.5 | 9.5 |
| Potassium titanyl phosphate (KTP) | 1.5 | 9.5 |
| L-phenylalanine L-phenylalaninium perchlorate | 1.4 | 7.4 |
| L-Asparaginium L-tartarate (AST) | 1.5 | 8.1 |

** Present work

### 3.8. Antibacterial Studies

Antibacterial activity is significantly influenced by any material with a size between 50 and 750 nm. Bacteria can grow on the surfaces of crystalline samples after they are harvested, and bacterial biofilms can form on the samples. To test this, an antibacterial activity study was performed on the grown GCCA crystalline sample, which was evaluated against two bacterial strains, E.coli and Staphylococcus aureus. Antibacterial activity was performed by agar diffusion method. Van der Watt *et al.*, 2001. The stock culture of bacteria (*K.Pnemoneae, Staphylococcus, Bacillus, E.coli*) were received by inoculating in nutrient broth media and grown at 37% for 18 hours. The agar plates of the above media were prepared. Each plates was inoculated with 18 hours old cultures the bacteria were swab in the sterile plates. Cut the

5 wells Pour the extract in ratio1 %, 0.1%, 0.01%, 0.001%. All the plates were incubated at 37$^{o}$C for 24 hours and the diameter of inhibition zone was noted in Cm.

**Table: Inhibition zone values of E.Coli and S.aureus on various concentrations of GCCA sample**

| **Concentration** | ***E.Coli*** | ***Staphylococcus aureus*** |
|---|---|---|
| 25 ul | 0.8 cm | 0.5 cm |
| 50 ul | 1.3 cm | 1.2 cm |
| 75 ul | 1.8 cm | 1.7 cm |
| 100 ul | 2.0 cm | 2.0 cm |
| STD | 2.2 cm | 1.8 cm |

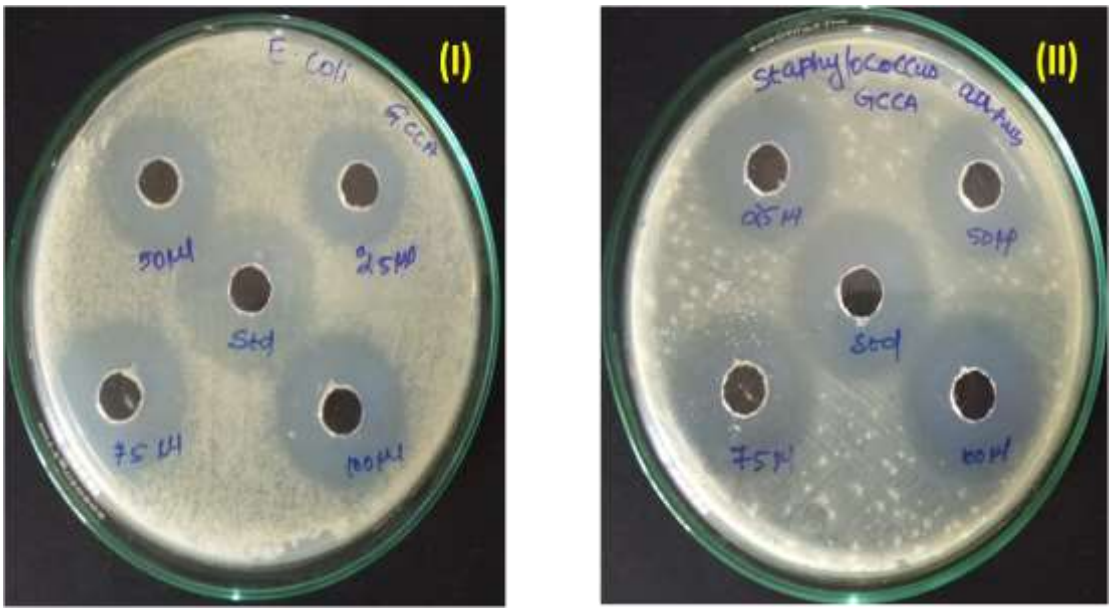


**Fig. 9. Antibacterial activity of GCCA Crystals (I) E.coli (II) Staphylococcus Aureus**

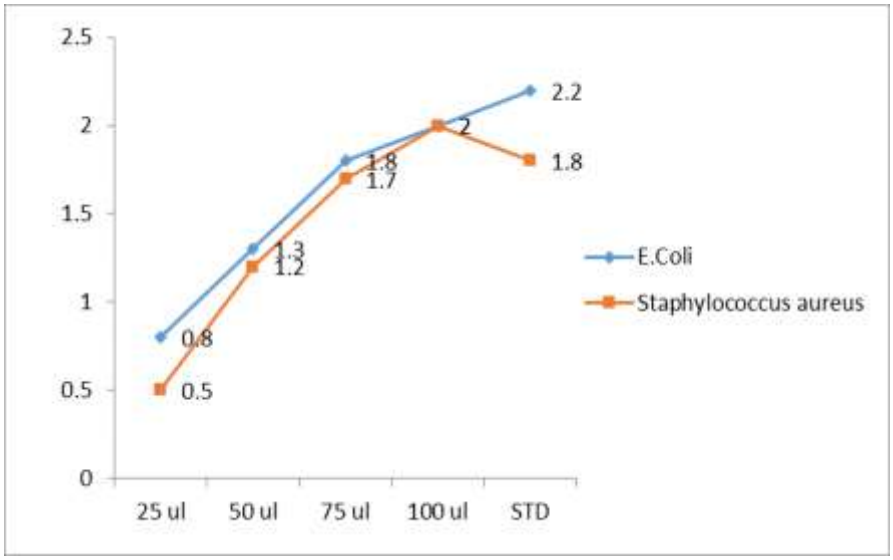


**Fig. 10 Inhibition zone variation of (I) E.coli (II) Staphylococcus Aureus**

The figure depicts the antibacterial activity of the grown sample against both gram negative and gram positive stains. After incubation around each well, the antibiotic zone scale was used to calculate the absence of bacterial growth around the zone of inhibition. The data suggest that the increased antibacterial activity of the GCCA sample against E.Coli and Staphylococcus aureus bacterial strains may be due to surface free energy, which determines bacterial adhesion onto crystal surfaces. Susceptible strains have a larger zone of inhibition, whereas resistant strains have a smaller zone of inhibition. [19]. The high antibacterial activity which has the ability to destroy the bacterial cells found in E.Coli the gram negative bacteria than S.aures, which may be due to hydrogen bonding interactions that effectively prevent biofilm related problems in the title GCCA sample which is suitable for biological applications [20].

**4. Conclusion**

Guanidinium Carbonate Crystals were grown in the Presence of Cyanoacetic acid act as a solvent by the Slow Evaporation technique at room temperature. The X-ray diffraction studies confirm the tetragonal structure of grown crystal and their space group is $P4_12_12$. The FT-IR study identified the presence of functional groups. From the UV-Visible spectrum of the GC Crystal shows low absorbance with cutoff wavelength is 239.46 nm and their optical bandgap is determined from optical absorption studies is found to be 5.34 eV. The microhardness studies confirmed that the GC crystal belongs to soft material category and suggest suitability of material in device fabrication. The LASER damage threshold valueis 9.5 GW/cm$^2$. The SHG efficiency is early 1.5 times greater than that KDP crystal. Hence one could confirm that the harvested GC crystals belongs NLO material. The antifungal activity of grown GC Crystal has ability to destroy the bacterial cells due to hydrogen bonding interactions that effectively prevent biofilm related problems, GC Crystal is suitable for biological applications like food sciences, medical sciences and agriculture.

**Acknowledgement**

The authors are grateful to the Management of The M.D.T Hindu College, Pettai, Tirunelveli, for providing to access the DST-FIST Sponsored Instrumentation Laboratory and Research facilities of the Department.

**References**

1. P.N.Prasad, D.J.Wollians, Introduction to Nonlinear Optical effects in Molecules and Polymers, Wiley-Interscience, New York 1991.
2. Nazirahmed, Ahmad.M.M., Kotru.P.N., Single crystal growth by gel technique and characterization of lithium hydrogen tartrate J.Crystal Growth 412 2015: pp.72-79, https://doi.org/10.1016/j.jcrysagro.2014.11.034.
3. T.Baraniraj, P.Philominathan, Growth and Characterization of organic nonlinear optical material:Benzilic acid, J.cryst.Growth 311(2009) 3849-3854.
4. V.Sivashankar, R.Siddheswaran, T.Bharathasarathi, P.Murugakoothan, Growth and Characterization of new semi organic nonlinear optical zinc guanidinium sulfate single crystal, J.Cryst.Gowth 311 (2009) 2709-2713.
5. Beatrice Fraboni, Alessandro Fraleoni-Morgera, Yves Geerts, Albero Morpurgo, Vitaly Podzorov, Organic Single Crystals: An Essential step to New Physics and higher performances of Optoelectronic Devices Adv.Fun,Mater,26(14) 2016. Pp2229-2232. https://doi.org/10.1002/adfm.201504924
6. A.Suvitha, P.Murugakoothan, Synthesis, growth, structural, spectroscopic and optical studies of semiorganic NLO crystal: zinc guanidinium phosphate, Spectrochim, ACta Part A 86(2012) 266-270.
7. https://dx.doi.org/10.1016/j.jjleo.2015.10.159
8. J.M.Adams, R.W.H.Small, The crystal structure of guanidinium carbonate, Acta Crystallogr, B30 (1974)2191.
9. R.K.Khanna, P.J.Miller, Spectrochim. Acta A26 (1970) 1667.
10. T.Arumanayagam, P.Murugakoothan, optical and electrical properties of a new organic nlo crystal: guanidinium 1-monohydragenetartrate 1-tartaric acid Optoelectron. Adv.Mater, 6(12) 2012: pp 263-265.
11. R. E. Denton, R. D. Campbell, S. G. Tomlin, J. Phys. D: Appl. Phys. 1972, 5, 852.
12. S.Ananthi, M.Rajalakshmi, T.S.Shyju, R.gopalakrishnan, Growth and Characterization of an aauct 4-aminobenzoic acid, J.Cryst.Growth 318 (2011)774-779.
13. B.Deepa, P.Philominathan, Optical, Mechanical and thermal behavior of Guanidinium Carbonate single crystal, Optik 127 (2016) 1507-1510
14. D.Sathya, V.Sivashankar, D.Prem Anand, R.Murugesan, Structural, optical, mechanical studies of Guanidine Tartrate single crystal, IJSRSET184166, 2018, pp 393-399
15. B.Deepa, P.Philominathan, Optical, Mechanical and thermal behavior of Guanidinium Carbonate single crystal, Optik 127 (2016) 1507-1510
16. J.Mary Linet, S.Jerome Das, Spectral, Thermal and Hardness Studies on

unidirectional grown dichloride diglycine zinc dehydrate single crystal, Physica B 406(2011) 836-840.

17. John Coates, Interpretation of Infrared Spectra, a Practical Approach, Coates Consulting, Newtown, USA.
18. V.V. Azarov, et al. J.Quantum Electron. (1985) 15, 89.
19. Geetha Palani, Arul H, Sengottain Shanmugan & Chithambaram V, *Materials Research Innovations,***25,** (2020), 331-337.
20. S.Anciya, A.S.I Joy Sinthiya, P. Selvarajan and R.Sree Devi, *Materials Today Proceedings* 49 (2022) 2276-2282.